



3D resistivity model of 1D vertical electrical sounding (VES) data for groundwater potential and aquifer protective capacity assessment: a case study

Kolawole Isaac Arowoogun¹ · Olawale Olakunle Osinowo²

Received: 5 June 2021 / Accepted: 31 July 2021 / Published online: 13 August 2021
© The Author(s), under exclusive licence to Springer Nature Switzerland AG 2021

Abstract

Assessment of groundwater potential and aquifer protection capacity is essential in proffering solution to groundwater exploration challenges and contaminants invasion into the aquifers. In this study, 3D resistivity model of one hundred and forty-three (143) VES data acquired along a grid layout was generated. The VES data were processed and interpreted quantitatively to obtain geo-electric parameters and longitudinal conductance. The geo-electric parameters, longitudinal conductance values and georeferenced geographic coordinates were gridded using 3D gridding algorithm to generate resistivity and longitudinal conductance distribution model for the study area. The 3D resistivity models were presented as resistivity distribution models, slices, and depth maps. The result reveals variable resistivity ranges from 50 to 2800 Ωm , and an observable low resistivity values (30–160 Ωm) occupying larger part of the study area. The northeastern portion of the distribution model shows an anomalous high resistivity range between 1000 and 2000 Ωm . The variation in resistivity distribution could be ascribed to the heterogeneity of basement complex rocks. The resistivity model further reveals low fracturing intensity across the area, and a low to moderate groundwater prospect. The longitudinal conductance distribution model classified the area into poorly protected zone (43%), moderately protected zone (50%) and excellent protective zones (7%). Thus, 3D subsurface resistivity model of 1D sounding data has proven to be suitable for groundwater potentiality mapping and overburden protective capacity assessment in basement terrain.

Keywords Electrical resistivity · Dar-Zarrouk parameter · Overburden · Contamination

Introduction

The global demand for clean and potable water is increasing due partly to skyrocketing population and socio-economic activities (Wada et al. 2010). The readily available water from surface sources such as lakes and rivers are prone to contamination. Thus, groundwater remains the most available and affordable freshwater source that can meet global water demand. It constitutes more than ninety percent

of the freshwater available on earth and occupies pore spaces and fracture zones within a geologic stratum (Todd 2004).

Typically, storage and flow of groundwater in basement complex terrain is dependent on the matrix of the structures in the area (Olorunfemi and Fasuyi 1993). As a result, groundwater availability in basement complex is unpredictable and highly confined to small areas, usually in fractured rocks (Osinowo and Olayinka 2012). Haphazard siting of boreholes without using a scientific approach has led to many poor or low yield borehole in some parts of Nigeria (Bayode et al. 2007). The unsystematic approach of borehole siting has adverse effect on the environment, as groundwater levels are lowered and causes degradation of water quality (Carter et al. 2014; Fashae et al. 2014). Hence, delineation of suitable groundwater zones could help in the appropriate planning and management of groundwater resources (Rao 2006).

Therefore, it is imperative to conduct a detailed examination before selecting a site for groundwater abstraction. For

✉ Kolawole Isaac Arowoogun
arowoogunkolawole@gmail.com;
akolawole1@student.gsu.edu

¹ Department of Geosciences, Georgia State University, Atlanta, GA, USA

² Department of Geology, University of Ibadan, Ibadan, Nigeria

this purpose, there are several geophysical techniques that have been used to probe the subsurface in the basement complex terrain. These methods range from traditional single point geophysical measurements to integrated approaches aimed at reducing ambiguity in geophysical interpretation. Traditional single point geophysical techniques such as electrical methods and electromagnetic methods have been the most widely applied (Pellerin 2002; Chegbeleh et al. 2009). The vertical electrical sounding (VES) has proven to be the most used electrical resistivity technique in delineating favorable areas for groundwater accumulations. Thus, selection of VES in this study is based on numerous case studies of its successful applications in groundwater exploration.

However, apart from challenges in identifying potential groundwater zones, aquifer contamination is another threat to provision of clean water. The occurrence of basement complex aquifers is rarely at considerable depth and are often vulnerable to the risk of groundwater contamination by leachate and contaminants percolating through the subsurface (Omosuyi 2010; Bayewu et al. 2018). It is essential to understand the protective nature of overburden covers in the area to reduce the risk of contamination.

The most adaptable of geophysical techniques in protective capacity study is the electrical resistivity method (Oni, et al. 2017; Adeyemo et al. 2017). Atakpo and Ayolabi (2009) applied vertical electrical sounding (VES) technique using Schlumberger array to determine the overburden protective capacity in six oil producing areas in Niger Delta. The calculated geo-electric parameters obtained in the study aids the assessment of the protective zones.

VES measurements are not directly used for contamination vulnerability assessment except priori information such as the borehole data which can reveal and complement the nature of the material delineated by the VES. The need for complementary information can be attributed to overlap of resistivity values (i.e., different geologic material can give rise to same signature). Geoelectric parameters obtained from VES are combined with other parameters to develop models to evaluate protective capacity.

These models are used to evaluate the protective cover of an aquifer. The most prominent models are the longitudinal conductance model (Udosen 2021), groundwater-overall lithology-depth (GOD) model (Oni et al. 2017), geo-electric layer susceptibility indexing (GLSI), susceptibility index (SI) and depth-recharge-aquifer media-soil media-topography-impact of vadose zone-hydraulic conductivity (DRASTIC) (Mclay et al. 2001).

DRASTIC method aids the assessment of aquifer vulnerability to contamination using measured parameters to define hydrogeological units influenced by contaminant transport processes. SI method was developed to assess vulnerability to agricultural contamination. GOD model is used in measuring the vulnerability of aquifer to vertical

percolation of pollutants. GOD model is developed based on three parameters namely groundwater occurrence, overall aquifer class and the depth of water table. The various models have proven to be effective in evaluating protective capacity of basement aquifers. For example, Oni et al. (2017) examine the comparison between three vulnerability assessment models on predicting aquifer protective capacity using GOD, GLSI and longitudinal conductance models. These techniques were successfully used in classifying the study area into different protective capacity regimes. Many other studies have also validated the successful applications of vulnerability models (Gogu and Dassargues 2000; Thirumalaivasan et al. 2003; Khemiri et al. 2013). However, it is noteworthy that vulnerability assessment parameters have built-in limitations and strengths (National Research Council 1993; Foster et al. 2002; Ghouili et al. 2021), and the ultimate choice of parameters used at any site is primarily a function of data availability, and the expertise of the interested party (Ghouili et al. 2021). The longitudinal conductance value was selected for aquifer vulnerability assessment in this study as it focuses on geophysical measurement, unlike the DRASTIC, SI and GOD methods that focuses on hydrogeologic based parameters (Mclay et al. 2001; Herbst et al. 2005).

This study therefore attempts to assess groundwater potential and aquifer protective capacity from 3D model of resistivity and longitudinal conductance values derived from gridded VES data in parts of Ibadan. The use of 3D modeling of VES data is to obtain geological information of the study area beyond the capability of traditional 1D sounding data which does not incorporate lateral and vertical distribution of resistivity.

Description and geology of the study area

The study area is located within the Ibadan metropolis and is bounded by latitudes $7^{\circ} 25' 00''$ and $7^{\circ} 28' 00''$ and longitudes $3^{\circ} 51' 00''$ and $3^{\circ} 55' 00''$ (Fig. 1). The weather condition in the area is characterized by an alternating seasonality (i.e., rainy, and dry seasons) typical of the West African Monsoon climate. The rainy season often begins in March and ends in October with a mean annual rainfall of about 1205 mm. The dry season commences in November and last till February (Egbinola et al. 2017). The area is drained by rivers and tributaries; the main river draining Ibadan are Ona River, Ogbere river and Ogunpa river. The rivers exhibit dendritic drainage patterns diagnostic of basement complex terrain. The mean annual surface temperature ranges from 18 and 37 °C with an annual mean surface temperature of 28 °C (Egbinola et al. 2017).

The geology of the study area falls within the basement complex rocks of the southwestern Nigeria which are

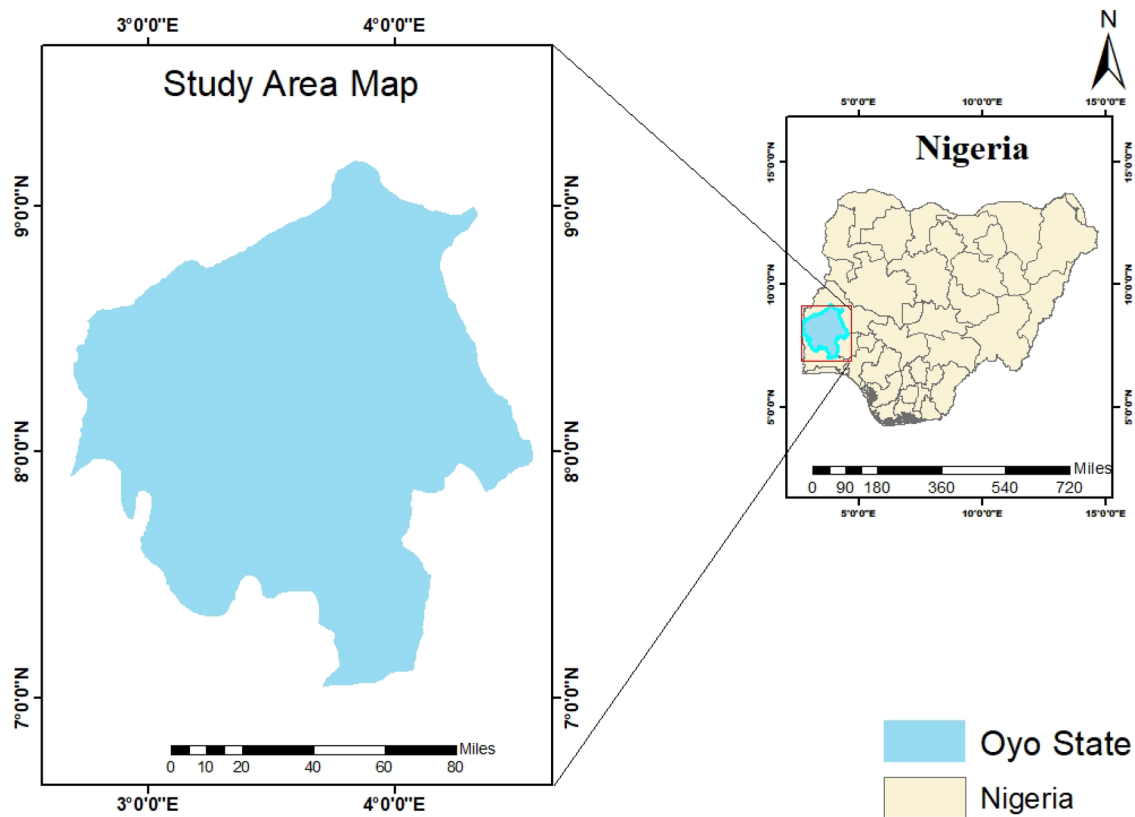


Fig. 1 Map of the study area

Precambrian to Lower Palaeozoic in age (Rahaman 1976). It also consists of the meta-sedimentary suites, Migmatite Gneiss Complex comprising the banded gneiss and the migmatite (Burke and Dewey 1972). These rocks are characterized by intrusion of pegmatite, quartz vein and dolerite dykes. Quartz-schist outcrops occur as long and relatively high ridges and pockets exposure of banded gneiss in the western and northern part. There are exposures of banded gneiss in the western and northern parts of Ibadan metropolis, some of which are intruded by veins and dykes.

Minor structures such as folds, shear zones, pinch and swell structures concordant and discordant quartz-veins, and quartzo-feldspathic intrusions are present in the banded gneiss. The rocks within the parts of Ibadan which constitute the study area are basically migmatite and banded gneiss, quartzite and quartz schist, and granite gneiss (Fig. 2).

Methodology

3D resistivity and longitudinal conductance modeling

3D resistivity model

To generate resistivity and longitudinal conductance model in this study. A grid layout of 10 by 15 VES stations were established in the east–west direction of the study area. The VES stations were well spread throughout the area to account for the complexity of the different rocks present in the study area (Fig. 3). The VES data were acquired using the Campus Tiger resistivity meter with a custom-built transmitter. The Schlumberger electrode array configuration was used with a minimum and maximum electrode spacing of 1–100 or 133 m. The individual VES stations are separated by approximately 100 m along the profile and 150 m across the established profile line to generate a grid.

One hundred and forty-three (143) VES stations were occupied in the area out of the one hundred and fifty 150 points defined on the grid, this is due to the inaccessibility of parts of the grid because of overflow of Eleyele rivers and its tributaries during the peak of rainy season when

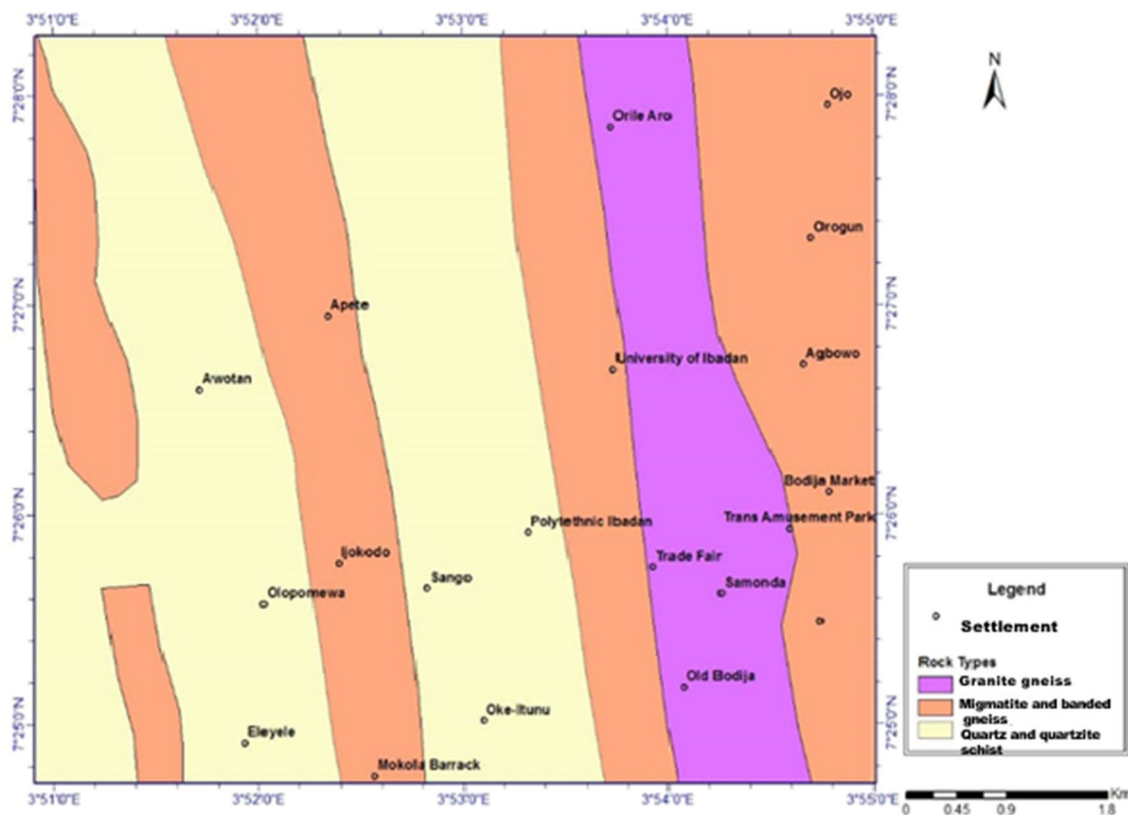


Fig. 2 Geological map of parts of Ibadan (Osinowo and Arowoogun 2021)

the fieldwork was conducted. The VES points could not be offset without distorting the geometry of the grid designed for 3D modeling purposes.

The resistivity data acquired was plotted against electrode spacing on a bi-log sheet using manual curve matching technique and subjected to computer-assisted iteration using the Winglink interpretation software to generate primary geo-electric parameters (i.e., layer resistivity and thickness).

Longitudinal conductance model

Longitudinal conductance value (S), a derivative of Dar-Zarrouk parameters (Maillet 1947; Zhody et al. 1974) was calculated using the ratio of thickness to geo-materials' resistivity as shown in Eq. 1.

$$S = \frac{h_1}{\rho_1} + \frac{h_2}{\rho_2} + \frac{h_3}{\rho_3} + \dots + \frac{h_n}{\rho_n} \quad (1)$$

where, $h_1, h_2, h_3,$ and h_n represent the thickness of individual layers and ρ_1, ρ_2, ρ_3 and ρ_n indicate the resistivity of the respective layers.

Longitudinal conductance aids in assessing the protection level of groundwater from migrating contaminants (Atakpo and Ayolabi 2009). The longitudinal conductance values

were used as an index to measure the study area's protective capacity utilizing a rating scale from Oladapo et al. (2004), as shown in Table 1.

The geo-electric parameters delineated from the VES data and the calculated second order geo-electric parameters, that is the longitudinal conductance, were geo-referenced using their geographic positioning system (GPS) coordinates. They were sorted into profiles and depths, and imported into OasisMontaj (Osinowo and Falufosi, 2018). The imported data were processed and subsequently used to generate 3D pseudo model for resistivity and longitudinal conductance distribution. The resulting model was smoothed to produce resistivity and longitudinal conductance model diagnostic of the study area. The processes involved in this study are summarized in the flow chart presented in Fig. 4.

Results and discussion

This section presents the result of modeling of the 1DVES data across the study area. They are presented as 3D resistivity distribution model, horizontal depth slices, section maps and 3D longitudinal conductance distribution models.

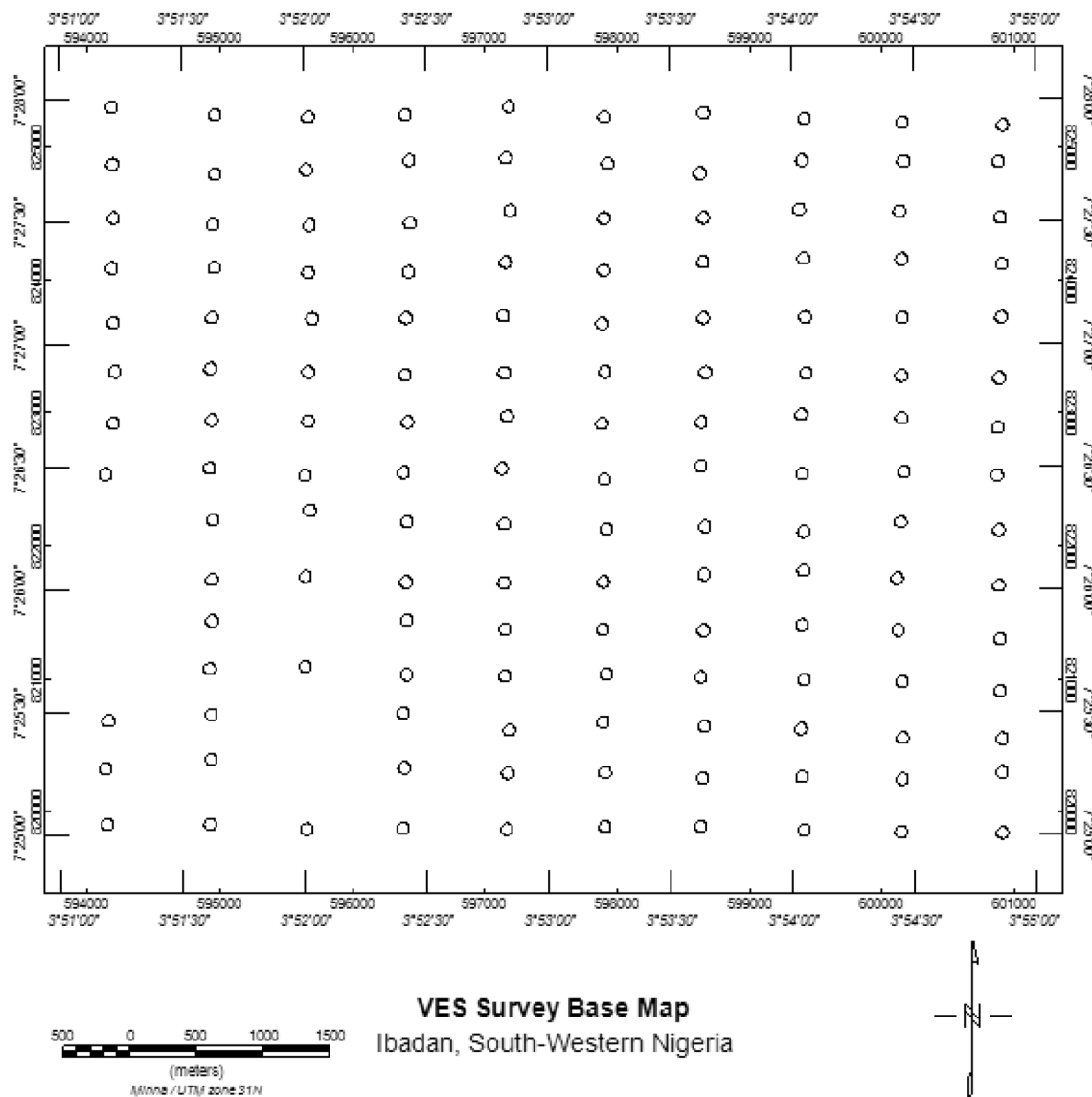


Fig. 3 VES point data grid showing the acquisition layout

Table 1 Longitudinal conductance/protective capacity rating scale (Oladapo et al. 2004)

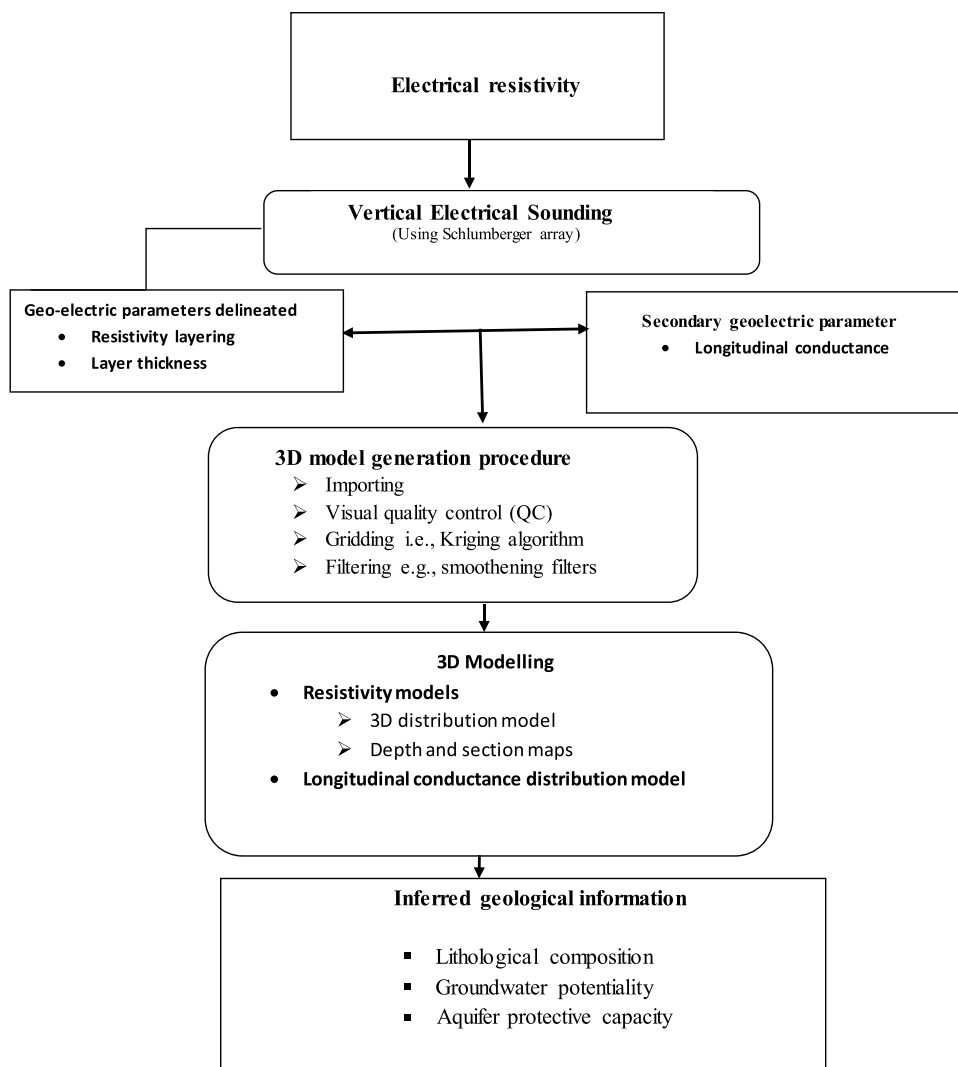
Longitudinal conductance (mhos)	Protective capacity rating
> 10	Excellent
5–10	Very good
0.7–4.9	Good
0.2–0.69	Moderate
0.1–0.19	Weak
< 0.1	Poor

3D resistivity model

The generated 3D resistivity distribution model generally shows distribution ground resistivity values across the study

area as well as variation with depth. The resistivity distribution model aggregates all the VES points on all profiles in the study area (Fig. 5). The 3D model shows resistivity values that range from 50 to 2800 Ωm (Fig. 5). Low resistivity value less than 160 Ωm dominates more than fifty five percent (55%) of the study area. The northeastern part of the area presents anomalous high resistivity values at the surface (2000 Ωm) which coincides with the occurrence of massive, unweathered outcrop of migmatite gneiss. The characteristic variable but low resistivity distribution (usually less than 100 Ωm) of the topsoil (just below the ground surface) indicates heterogeneity of the layer and can be attributed to the variable composition of the topsoil in the study area. The topsoil consists of unsaturated clay/sandy, clay/clayey sand, and lateritic sand. The marked portion labeled A (Fig. 4)

Fig. 4 Flowchart illustrating the processes in generating 3D resistivity and longitudinal conductance distribution model from VES data in the study area



represent the low resistivity ($< 165 \Omega\text{m m}$) part of the study area, while the labeled part, B and C is intermediate and high in resistivity distribution, respectively.

3D resistivity depth section model

The 3D resistivity model generated different iso-depths layer maps at 20 m intervals (0, 20, 40, 60, 80 and 100 m) as shown in Fig. 6. The resistivity distribution just below the surface represents the ground surface that revealed the variable composition of topsoil in the area. The topsoil is not of significant interest in groundwater exploration, although it is of substantial interest in protective capacity assessment.

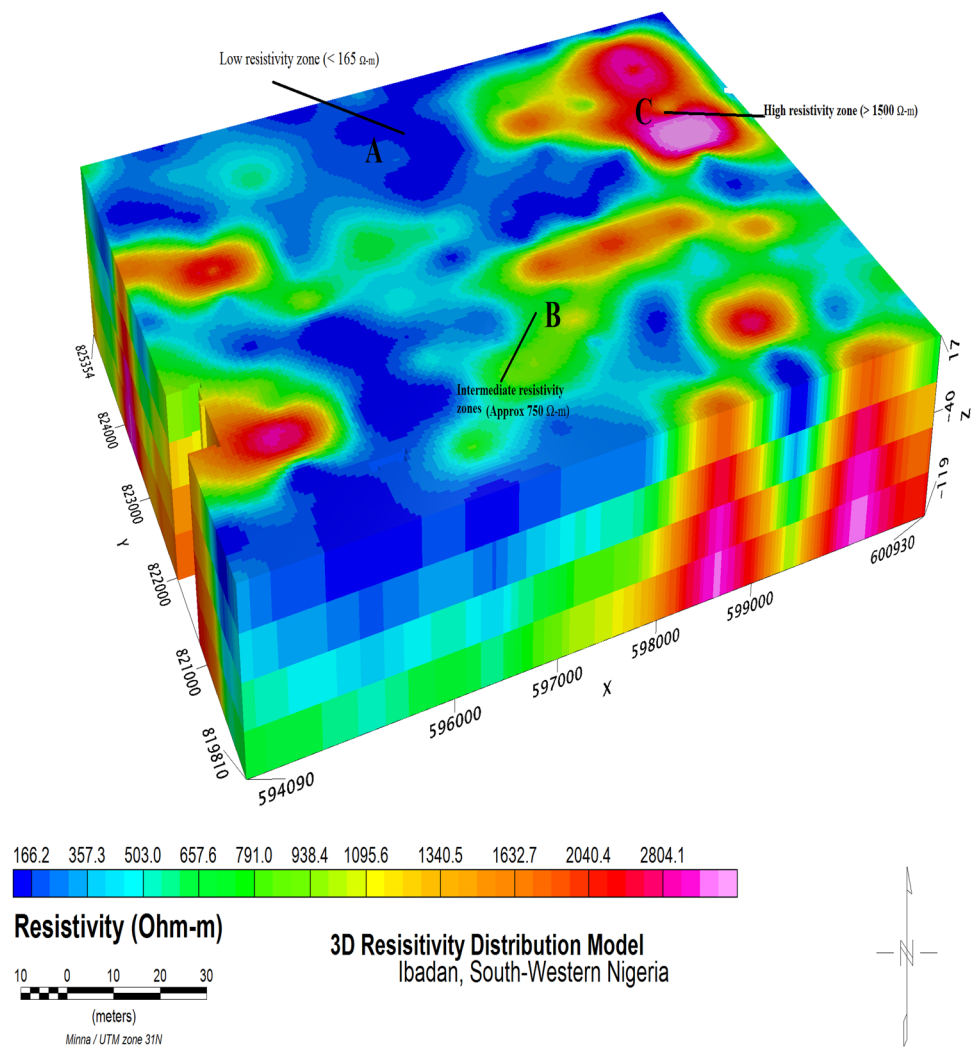
The iso-depth layer resistivity distribution map (Fig. 6) at 20 m generally indicates resistivity values that range from 150 to 200 Ωm . The relatively low resistivity ($< 165 \Omega\text{m}$) distribution that dominates the layer, except for isolated higher values at the fringes could likely be associated in part, with increase in moisture content down the weathered

profile as well as the saturated saprolite. The resistivity distribution at 20 m depth ranges from 300 to 2800 Ωm within the central part accounting for more than 35% areal coverage characterized with higher resistivity distribution, more than 500 Ωm . This indicates possible decrease in groundwater saturation which may be associated with decrease in fracture intensity with depth.

Resistivity distribution slice at 40 m (Fig. 6) has visual expression of the resistivity that is not too dissimilar from that at 10 m except for the sharp increase of the low resistivity zone at the small portion located in central part of the study area, which could easily be linked to compaction at depth. Other areas have higher resistivity value corresponding to occurrence of unfractured basement.

The resistivity model sections at depths of 60 m and 80 m (Fig. 6) are similar in terms of the visual resistivity signature. The resistivity signature generally increases with depth across the imaged depths ($> 400 \Omega\text{m}$). Part of the central and southwest of the study area present intermediate resistivity

Fig. 5 3D resistivity distribution model of the study area



value around 600 Ωm . This suggests possible significantly water saturation likely associated with high degree of fracturing. This depth range is appropriate target for groundwater resource development. The relatively high resistivity zone in the northeastern part of the study area coincides with occurrence of outcrop of basement crystalline rock and gained prominence with depth, as the resistivity values remains higher than the surroundings. The northwestern, northeastern, and central parts display relatively high resistivity values ranging from 1000 to 2850 Ωm which possibly suggest that the basement rocks in such areas are not fractured at depth and thus poorly saturated with groundwater. The resistivity distribution model section at depth of 100 m (Fig. 6.) shows values that vary from 1000 to 2900 Ωm . The dissimilar response observed from the 3D resistivity model (at 100 m) in the area can be interpreted in terms of varying electrical resistivity response to diverse rock types, saturation degree, and diverse geological conditions at depth.

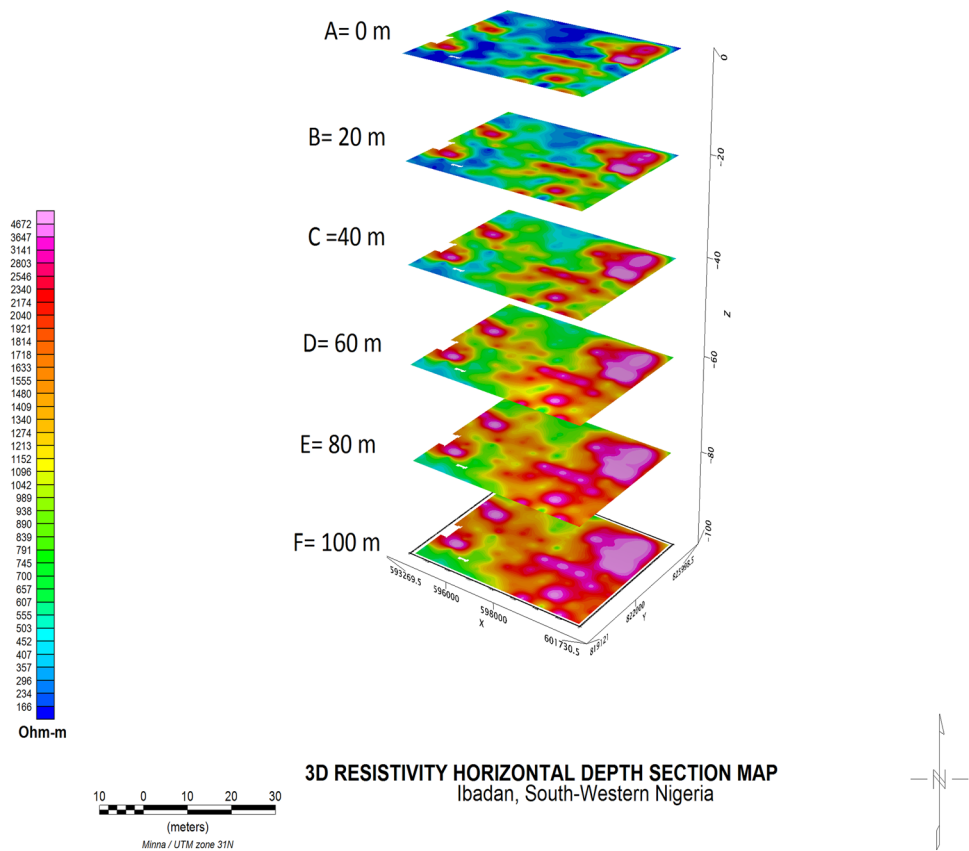
The region of low resistivity on the 3D model is a fractional part of the whole resistivity depth section. Only a

smaller part of the area displayed relatively low resistivity compared to the other part. The fractional resistivity denotes that basements in the area are fractured at depth. Given the depth of occurrence of the delineated fracture, such deep fractures can be potential targets for groundwater exploration. The presence of fracture is limited to that zone which further prove that fractures in basement rocks are usually not interconnected and often develop due to faulting. The significantly high resistivity distribution around 100 m depth indicate occurrence of fresh basement rocks at depth. Generally, the horizontal resistivity depth section shows an increasing trend of resistivity with depth in the subsurface, as porosity gradually decreases with depth of burial.

3D resistivity distribution along N–S and E–W directions

The resistivity distribution model of the study area was extracted across the N–S direction and the sections are

Fig. 6 3D resistivity model depth section map



perpendicular to the x -axis (easting) direction) as presented in Fig. 7.

The resistivity distribution along the N–S direction generally present values which range from 50 to 2800 Ωm (Fig. 7). The sections also indicate the subsurface subdivision into two geo-electric horizons, namely the overburden and fresh (unweathered) basement. The overburden resistivity ranges from 70 to 700 Ωm , while the fresh basement has resistivity values ranging from 1000 to 2900 Ωm . The overburden thickness is highest in the northwest (NW) and increases along the southeast (SE) direction. The area underlain by migmatite gneiss is observed to present relatively high resistive values thus indicating relatively low degree of weathering which resulted in thin overburden thickness. The northwest portion with high overburden has potential for groundwater exploration while areas of thin overburden potentially depict low groundwater potential.

The E–W section map of the resistivity model is shown in Fig. 8. The locations are perpendicular to the northing's direction (Y axis). The E–W section (Fig. 8) presents relatively low resistivity distribution ($< 100 \Omega\text{m}$). The second horizon in the sections shows a high degree of fracturing with a resistivity value more than 500 Ωm . The basement rock has resistivity values varying from 1000 to 3680 Ωm . The right end of the section shows an anomalously high

resistivity value of about 3000 Ωm . These areas coincide with outcrops' exposure and indicate a relatively shallow fresh basement.

Figure 9 combines both N–S and E–W direction on a single plane. The low resistivity portion of the near-surface was only observed on the NE–SW diagonal. The sections show the differentiation into predominantly two mappable geo-electric horizons, namely the overburden and the fresh basement. The overburden's resistivity values range from 60 to 800 Ωm , while that of the fresh basement ranges from 1000 to 3900 Ωm .

The resistivity at the central part of the area is low at depth, and this suggests high degree of saturation or the presence of weathered regolith. This area can be exploited for groundwater purposes.

3D longitudinal conductance model

The 3D longitudinal conductance distribution model of the study area derived from procedure described in “3D Resistivity and longitudinal conductance modeling” is presented in Fig. 10.

Longitudinal conductance (S) model of the study area provide insight into the protective nature of the overburden and groundwater potentiality of the study area since low

Fig. 7 3D resistivity model (N–S) section map

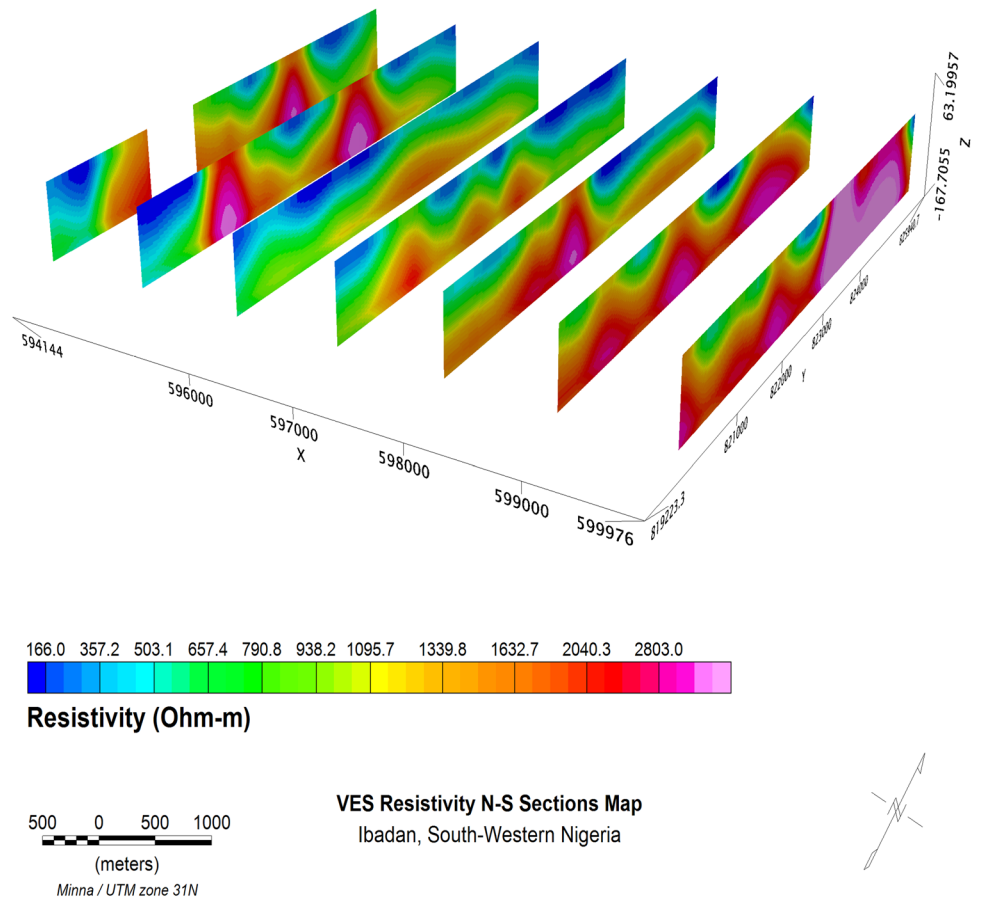


Fig. 8 3D resistivity model (E–W) section map

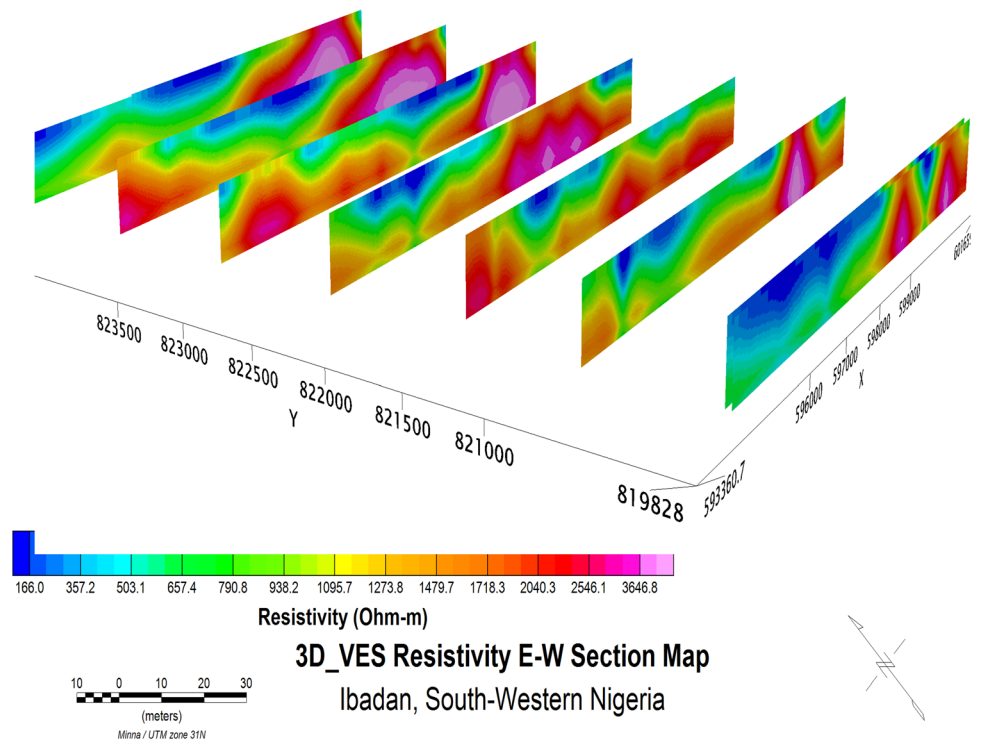
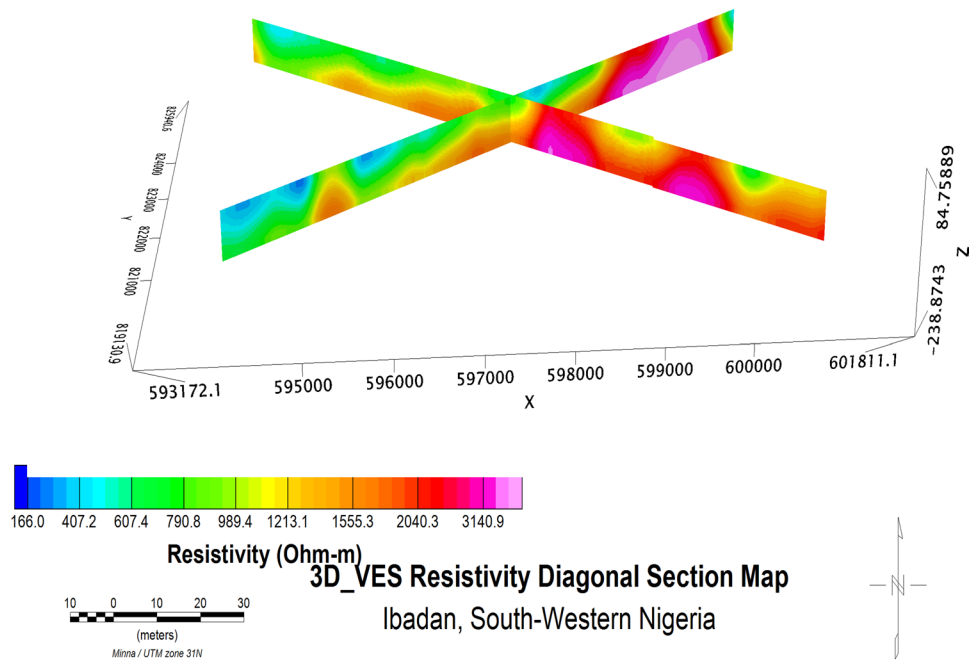


Fig. 9 3D resistivity diagonal (NE–SW and NW–SE) section map

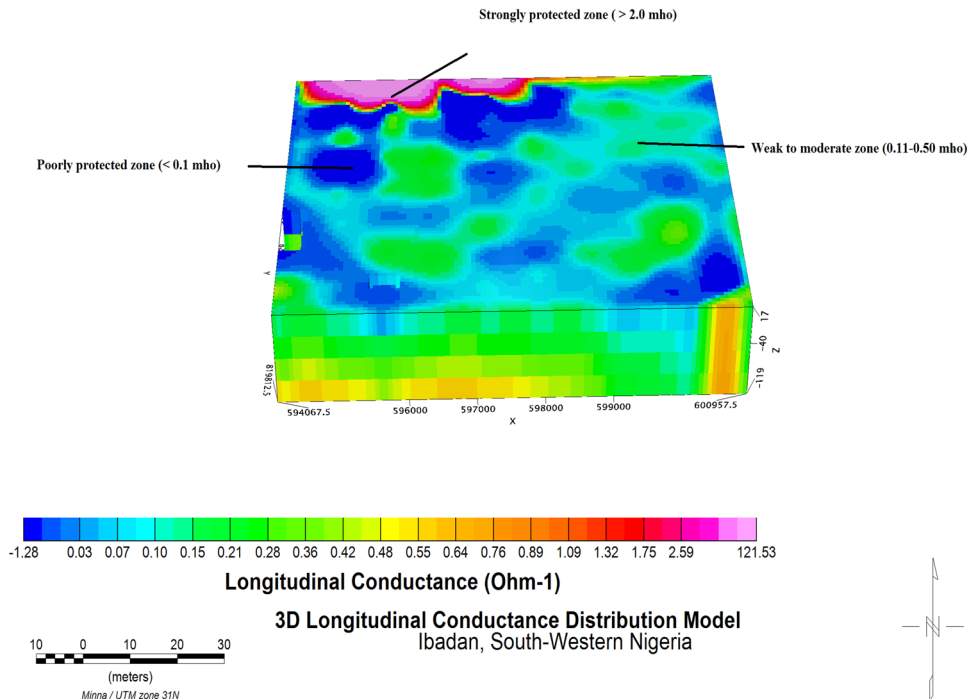


longitudinal conductance indicate that aquiferous zones has low clay unit and high permeability (Hassan 2018). From Fig. 9, the blue color represent area with low longitudinal conductance rating, the green color represent moderate longitudinal values rating while the red color represent areas with high longitudinal conductance rating. The 3D longitudinal conductance value of the study area was classified

into protective units using the ratings presented by Oladapo et al. (2004).

The longitudinal conductance model of areas with low protective capacity, i.e. (< 0.1 mho) constitutes approximately forty-three percent (43%) of the study area. Areas with longitudinal conductance values ranging from (0.20–0.5 mhos) are classified to have moderate protection capacity and occupy about fifty percent (50%) of the study

Fig. 10 3D longitudinal conductance distribution model of the area



area. The northwestern part of the study area is characterized by high longitudinal conductance value greater than 10 mhos. This area representing about seven percent (7%) of the study area, has strong protective capacity.

The qualitative interpretation of the longitudinal conductance models shows that large portion of the area are moderately protected which implies that the aquifer in the area has moderate protective cover from contamination. Only a fractional part of the studied area can be described as strongly protective zone. Thus, aquifers in the area can be broadly classified as moderate to weak protected.

Areas of low conductance values (in blue color) represent areas with high groundwater prospect because large longitudinal values are diagnostic of high aquifer hydraulic conductivity. Conversely, areas of high longitudinal conductance value represent extremely low areas of groundwater potential, since large longitudinal values can indicate high clay unit. From the longitudinal conductance model, about fifty percent of the study area coincides with areas of moderate groundwater potential. Generally, the study area can be classified based on the longitudinal conductance model as moderate in groundwater potential and moderately protected from surface contamination.

Conclusion

This study assesses groundwater potential and aquifer protective capacity from 3D modeling of resistivity data in a basement complex terrain. It is necessitated because the study area is an urban area with dense population, and as such demand for clean water is on the rise. The study attempt to generate 3D resistivity model and longitudinal conductance model from 1D sounding data. The results presented as sections and depth maps provides valuable information about the lithological composition, structural disposition and ultimately provides insight into the groundwater potentiality. The longitudinal conductance model generated from the VES data also serves as a framework to classify the area into groundwater potential and different protective capacity ratings. The 3D modeling of VES data has proven to be capable of imaging the subsurface and provide useful information about groundwater potential and aquifer protection capacity in the study area. The information generated from 3D model of resistivity sounding and the longitudinal conductance values agrees in terms of groundwater potentiality of the study area which classifies half of the study area as moderate in terms of groundwater potential and protective capacity. This inference buttresses the low to moderate potentiality of basement terrain and the moderate protective capacity in hard rock terrains of Nigeria which have been reported from past research. Therefore, the information generated in this study can be used in the planning of groundwater site selection

and sustainable management of groundwater resources in the study area and the method can be adapted into different geological environment considering the complexity of local and regional geology.

Funding This study was funded by the authors and did not enjoy funding either as grant or aid from any funding agent.

Declarations

Conflict of interest There is no conflict of interest.

Compliance with ethical standards This study was carried out in compliance with ethical standard, no violation of ethical standard.

Non-ethical approval Not applicable.

References

- Adeyemo IA, Omosuyi GO, Ojo BT, Adegunle A (2017) Groundwater potential evaluation of a typical basement complex environment using GRT index—a case study of Ipinisa-Okeodu Area, Akure. *J Geosci Environ Prot Sci Res* 5(3):240–251
- Atakpo EA, Ayolabi EA (2009) Evaluation of aquifer vulnerability and the protective capacity in some oil producing communities of western Niger Delta. *J Environ* 29:310–317
- Bayewu OO, Oloruntola MO, Mosuro GO, Laniyan TA, Ariyo SO, Fatoba JO (2018) Assessment of groundwater prospect and aquifer protective capacity using resistivity method in Olabisi Onabanjo University campus, Ago-Iwoye, Southwestern Nigeria. *NRIAG J Astron Geophys* 7(2):347–360. <https://doi.org/10.1016/j.nrjag.2018.05.002> (ISSN 2090-9977)
- Bayode S, Ojo JS, Olorunfemi MO (2007) Geophysical exploration for groundwater in Ejigbo and its environs, Southwestern Nigeria. *Global J Geol Sci* 5(1):41–49
- Burke KC, Dewey FJ (1972) Orogeny in Africa in *Afr Geol* Ibadan. Ibadan Univ Press, pp 583–608
- Carter R, Chilton J, Danert K, Olschewski A (2014) Siting of drilled water wells—a guide for project managers, rural water supply network (RWSN), St Gallen, Switzerland
- Chegbelah LP, Akudago JN, Makoto E, Samuel N (2009) Electromagnetic geophysical survey for groundwater exploration in the voltian of Northern Ghana. *J Environ Hydrol* 17:1–16
- Egbinola CN, Olaniran HD, Amanambu AC (2017) Flood management in cities of developing countries: the example of Ibadan Nigeria. *J Flood Risk Manag* 10(2017):546–554
- Fashae OA, Tijani MN, Talabi AO (2014) Delineation of groundwater potential zones in the crystalline basement terrain of SW-Nigeria: an integrated GIS and remote sensing approach. *Appl Water Sci* 4:19–38. <https://doi.org/10.1007/s13201-013-0127-9>
- Foster SSD, Hirata RCA, Gomes D, Eli D (2002) Groundwater quality protection. A Guide for Water Service Companies, Municipal Authorities and Environment Agencies 002. World Bank, Washington <https://doi.org/10.1596/0-8213-4951-1>
- Ghouili N, Jarraya-Horriche F, Hamzaoui-Azaza F, FaouziZaghrarni M, Ribeiro L, Zammouri N (2021) Groundwater vulnerability mapping using the Susceptibility Index (SI) method: Case study of Takelsa aquifer, Northeastern Tunisia. *J Afr Earth Sci* 173:104035
- Gogu R, Dassargues A (2000) Current trends and future challenges in groundwater vulnerability assessment using overlay and index

- methods. *Environ Geol* 39:549–559. <https://doi.org/10.1007/s002540050466>
- Hasan M, Shang Y, Akhter G, Jin W (2018) Geophysical assessment of groundwater potential: 317 a case study from Mian Channu Area, Pakistan. *Groundwater* 56:783–796. <https://doi.org/10.1111/gwat.12617>
- Herbst M, Hardelauf H, Harms R, Vanderborght J, Vereecken H (2005) Pesticide fate at regional scale: development of an integrated model approach and application. *Phys Chem Earth Parts A/b/c* 30(8–10):542–549
- Khemiri S, Khemiri KS, A. Khnissi BA, Alaya S, Saidi F, Zargrouni, (2013) Using GIS for the comparison of intrinsic parameter methods assessment of groundwater vulnerability to pollution in scenarios of semi-arid climate. The case of fousana groundwater in the central of Tunisia. *J Water Resour Prot* 2013:835–845
- Maillet R (1947) The fundamental equations of electrical prospecting. *Geophysics* 12:527–556
- McLay CDA, Dragte R, Sparlin G, Selvarajah N (2001) Predicting groundwater nitrate concentrations in a region of mixed Agricultural land use: A comparison of three approaches. *Environ Pollut* 115:191–204
- National Research Council (1993) Ground Water Vulnerability Assessment: Predicting Relative Contamination Potential Under Conditions of Uncertainty. Washington, DC: The National Academies Press. <https://doi.org/10.17226/2050>
- Oladapo MI, Mohammed MZ, Adeoye OO, Adetola BA (2004) Geoelectrical investigation of the Ondo state housing corporation estate Ijapo Akure, Southwestern Nigeria. *J Min Geol* 40(1):41–48
- Olorunfemi MO, Fasuyi SA (1993) Aquifer types and the geoelectric/hydrogeologic characteristics of part of central basement terrain of Nigeria (Niger State). *J Afr Earth Sci* 16:309–317. [https://doi.org/10.1016/0899-5362\(93\)90051](https://doi.org/10.1016/0899-5362(93)90051)
- Omosuyi GO (2010) Geo-electric assessment of groundwater prospect and vulnerability of overburden aquifers at Idanre Southwestern Nigeria. *Ozean J Appl Sci.* 3(1):19–28
- Oni TE, Omosuyi GO, Akinlalu AA (2017) Groundwater vulnerability assessment using hydrogeologic and geo-electric layer susceptibility indexing at Igbara Oke, Southwestern Nigeria. *NRIAG J Astron Geophys* 6:452–458
- Osinowo OO, Olayinka AI (2012) Very low frequency electromagnetic (VLF-EM) and Electrical resistivity (ER) investigation for groundwater potential evaluation in a Complex geological terrain around the Ijebu-Ode transition zone, southwestern Nigeria. *J Geophys Eng* 9(4):374–396. <https://doi.org/10.1088/1742-2132/9/4/374>
- Osinowo OO, Falufosi MO (2018) 3D Electrical resistivity imaging (ERI) for subsurface evaluation in pre-engineering construction site investigation. *NRIAG J Astron Geophys* 7:309–317
- Osinowo OO, Arowoogun KI (2021) A multi-criteria decision analysis for groundwater potential evaluation in parts of Ibadan, southwestern Nigeria. *Appl Water Sci* 10:228. <https://doi.org/10.1007/s13201-020-01311-2>
- Pellerin L (2002) Applications of electrical and electromagnetic methods for environmental and geotechnical investigations. *Surv Geophys* 23:101–132
- Rahaman MA (1976) A review of the basement geology of Southwestern Nigeria. In: Kogbe CA (ed) *Geology of Nigeria*. Elizabethan Publishing Co., pp 41–48
- Rao NS (2006) Groundwater potential index in a crystalline terrain using remote sensing data. *Environ Geol* 50:1067–1076
- Thirumalaivasan D, Karmegam M, Venugopal K (2003) AHP-DRAS-TIC: software for specific aquifer vulnerability assessment using DRASTIC model and GIS. *Environ Model Softw* 18(7):645–656. [https://doi.org/10.1016/S1364-8152\(03\)00051-3](https://doi.org/10.1016/S1364-8152(03)00051-3) (ISSN 1364-8152)
- Todd DK (2004) *Ground water hydrology*. Wiley, New York
- Udosen NI (2021) Geo-electrical modeling of leachate contamination at a major waste disposal site in south-eastern Nigeria. *Model Earth Syst Environ.* <https://doi.org/10.1007/s40808-021-01120-9>
- Wada Y, Van Beek PH, Van KC, Reckman WT, Bierkens MF (2010) Global depletion of groundwater resources. *Geophys Res Lett*
- Zohdy AAR, Eaton GP, Mabey DR (1974) *Application of surface geophysics to groundwater investigations: techniques of water resources investigation of the United Geophysical Survey Book*. United States Government Printing Office, Washington, pp 42–55

Publisher's Note Springer Nature remains neutral with regard to jurisdictional claims in published maps and institutional affiliations.